Biological Trace Element Research (2022) 200:2948–2962
https://doi.org/10.1007/s12011-021-02868-y

Green Synthesis of Selenium Nanoparticles Mediated by *Nilgirianthus ciliates* Leaf Extracts for Antimicrobial Activity on Foodborne Pathogenic Microbes and Pesticidal Activity Against *Aedes aegypti* with Molecular Docking

Krishnan Meenambigai[1] · Ranganathan Kokila[1] · Kandasamy Chandhirasekar[1] · Ayyavu Thendralmanikandan[1] · Durairaj Kaliannan[2] · Kalibulla Syed Ibrahim[3] · Shobana Kumar[4] · Wenchao Liu[5] · Balamuralikrishnan Balasubramanian[6] · Arjunan Nareshkumar[1]

Received: 26 May 2021 / Accepted: 3 August 2021 / Published online: 24 August 2021

Abstract

The present study deals with the synthesis of selenium nanoparticles (SeNPs) using *Nilgirianthus ciliatus* leaf extracts, characterized by UV–Vis spectrophotometer, XRD, FTIR, FE-SEM, HR-TEM, DLS, and zeta potential analysis. The antimicrobial activity against *Staphylococcus aureus* (MTCC96), *Escherichia coli* (MTCC443), and *Salmonella typhi* (MTCC98) showed the remarkable inhibitory effect at 25 µl/mL concentration level. Furthermore, the characterized SeNPs showed a great insecticidal activity against *Aedes aegypti* in the early larval stages with the median Lethal Concentration (LC_{50}) of 0.92 mg/L. Histopathological observations of the SeNPs treated midgut and caeca regions of *Ae. aegypti* 4th instar larvae showed damaged epithelial layer and fragmented peritrophic membrane. In order to provide a mechanistic approach for further studies, molecular docking studies using Auto Dock Vina were performed with compounds of *N. ciliatus* within the active site of AeSCP2. Overall, the *N. ciliates* leaf-mediated biogenic SeNPs was promisingly evidenced to have potential larvicidal and food pathogenic bactericidal activity in an eco-friendly approach.

Keywords *Nilgirianthus ciliates* · Selenium nanoparticles · *Aedes aegypti* · Foodborne pathogens · In silico docking

Introduction

Mosquitoes are quarter-inch culicid who threaten three-quarter *Homo sapiens*. They carry various pathogens that caused diseases like dengue, chikungunya, yellow fever, West Nile fever, malaria, and filariasis worldwide [1–4]. Globally, 0.5 million people are infected, and 3.9 billion people are at risk of malarial dengue infection in around 128 countries [5, 6]. *Aedes aegypti* is the main vector of dengue and container-inhabiting species, where the immature do thrive in human-made habitats even with minimum available nutrients [7, 8]. The adult females of this species mostly depend on human beings for their food. The vector mosquito carries the pathogen in its saliva and transmits them during injection of its mouthparts for a blood meal [9, 10]. The lack of efficient drugs in eliminating the dengue virus and its capability to flourish during favorable conditions have provoked the researcher for alternative disease management programs, especially the vector control programs [11].

Balamuralikrishnan Balasubramanian is equally considered as first author.

✉ Balamuralikrishnan Balasubramanian
bala.m.k@sejong.ac.kr; geneticsmurali@gmail.com

✉ Arjunan Nareshkumar
naresh@periyaruniversity.ac.in

[1] Department of Zoology, School of Life Sciences, Periyar University, Salem 636011, India

[2] Department of Environmental Science, School of Life Sciences, Periyar University, Salem 636 011, India

[3] PG and Research Department of Botany, PSG College of Arts & Science, Coimbatore 641 014, Tamil Nadu, India

[4] Department of Zoology, Sri GVG Visalakshi College for Women, Udumalpet, Tamil Nadu, India

[5] Department of Animal Science, College of Coastal Agricultural Sciences, Guangdong Ocean University, Zhanjiang 524088, People's Republic of China

[6] Department of Food Science and Biotechnology, College of Life Sciences, Sejong University, Seoul, South Korea

Chemical control of the vector mosquitoes has become less effective due to the development of resistance in the vector populations and the synthetic chemicals also has severe effects on non-target organisms including human being [12]. The utilization of synthetic insecticides also leads to adverse environmental effects, including climate change and global warming [13]. Various nanoparticles such as gold, silver, titanium, and selenium were used extensively in mosquito control programs [14–16]. Cholesterol is vital for insects' growth and development and even to reproduce, but they cannot synthesize cholesterol de novo [17, 18]. A nonspecific intracellular lipid carrier Sterol Carrier Protein-2 (SCP-2) was expressed throughout the animal kingdom, including mosquitoes [19]. The *Ae. aegypti* SCP-2 (AeSCP2) has been reported to play a crucial role in cholesterol and fatty acid uptake in the midgut in both larval and adult mosquitoes [20]. Few studies have targeted that the AeSCP2 for developing new insecticides that prevent cholesterol biosynthesis in *Ae. aegypti* [21, 22]. Hence, the present study aims to target the cholesterol transport pathway associated with AeSCP2, which could be an alternative target for developing specific mosquitocidal agents. Hence, vector control by novel environment-friendly techniques and pesticides of natural origin are highly focused and given much attention at present.

Pathogenic foodborne microbes such as *Staphylococcus aureus*, *Escherichia coli*, and *Salmonella typhi* account for more than 50% of infectious diseases and are a primary causative agent in deadly human diseases that affect millions of people annually [23, 24]. Bacterial pathogens lead among the microbial pathogens in causing infection leading to death, disability, and socioeconomic burden [25]. Foodborne diseases are one of the fundamental health problems around the world population. Developed and developing countries are highly prone to these foodborne diseases affecting around 30% of the world population every year [26]. The primary source for these disease-causing pathogens is food-processing contaminants, packages, and storage in restaurants, supermarkets, or homes lacking proper food handling techniques [27, 28]. The pathogens that invade the food were opportunistic, establishing their colony leading to food spoilage and food poisoning. Though there was a dramatic development in the medical and pharmacological fields in recent years, the foodborne diseases mediated by few species such as *S. aureus* and *S. typhi* could lead to death [29]. These pathogens causing foodborne infections could lead to infertility in women, urinary tract infections, bone and joint infections, skin problems, and many other diseases [30]. The emergence of multi-drug resistant bacteria is one of the major causes of an increasing number of deaths [31]. Hence, the formulation of novel, effective, eco-friendly drugs is the most need of the hour. The advancement of green nanotechnology will attribute the solution for vector as well as the bacteria controlling policy. Nanoparticles have added significant interest to researchers in recent decades due to their exclusive structural, electronic, optical, and magnetic properties, which have a wide range of applications, including medicine and biology [2, 32].

Selenium is an essential trace element with fundamental roles in human health and the deficiency leads to diseases [33]. Selenium nanoparticles (SeNPs) are biologically more active than the organic and inorganic selenium. It has relatively larger applications, including medicine and health care products [34]. The SeNPs can be biologically synthesized by using extracts of plant parts. The active principles of plant compounds act as eco-friendly reducing and capping agents as well [35]. Researchers were still using many plants for the synthesis of SeNPs [36–38]. The *N. ciliatus* (Nees) Bremek (Syn. *Strobilanthes ciliatus* Nees) is a slender, aromatic shrub of the *Acanthaceae* family used extensively in Ayurveda [39]. The significance of this plant was that all parts were medicinally important [40]. Researchers confirmed that the presence of alkaloids, flavonoids, saponins, proteins, tannins, lupeol, betulin, stigmasterol, and stigmasterol glucopyranoside could reduce selenium ions for the formation of SeNPs as well as cap the nanoparticles avoiding further agglomeration [41, 42].

Therefore, the focal aim of this present investigation was to utilize *N. ciliatus* leaves for SeNP synthesis and analyzed for their potential properties of antibacterial and insecticidal activities. The antibacterial activity was analyzed against foodborne pathogens such as *S. aureus* (MTCC 96), *E. coli* (MTCC 443), and *S. typhi* (MTCC 98). The insecticidal activity and toxicity bioassay were analyzed against the dengue vector, *Ae. aegypti* with computational perspectives of layer-specific study, and fascinatingly, the vectors are directly collected from the field. Additionally, histopathological observations on the mosquito immature are also performed to explore the mode of action of the biologically synthesized SeNPs at the cellular level.

Materials and Methods

Preparation of *N. ciliates* Aqueous Extract

The *N. ciliates* (PU-ZOO-MP06-2015) leaves were collected from Siddha Garden, Mettur, Salem, Tamil Nadu, India. The freshly collected leaves were washed by water, allowed to be dried at room temperature (30 ± 2 °C) and followed by grinding into a fine powder using an electric blender. About 5 g of the leaf powder were mixed with 100 mL of sterile distilled water and boiled at 110°C for 10 min in a 250-mL Erlenmeyer flask. The solution was filtered through Whatman

filter No. 1 filter paper, and finally, the filtrate was stored at 4°C for further analysis and used within a week.

Biosynthesis of SeNPs

Selenious acid (30 mM) used as a precursor was mixed with 10 mL of the leaf extract. To this mixture, 40 mL of ascorbic acid (40 mM) was additionally added as reduction persistence. This blended mixture was then incubated at room temperature (30 ± 2°C) for 24 h. Later, the mixture color changed, and then the mixture was centrifuged at 9660 *g* for 30 min [43]. The collected pellets were subjected to washing by re-suspension in de-ionized water followed by centrifugation at 9660 *g* for 10 min to remove possible organic contamination present in nanoparticles. Finally, the pellet was freeze-dried into its powder form using a lyophilizer.

Characterization of the SeNPs

The synthesized SeNPs were characterized by UV–Visible spectroscopy (Shimadzu-1800, China). The phase formation and crystalline nature of the SeNPs were examined by a Rigaku X-ray diffractometer (XRD) at a voltage of 45 kV with Cu-Kα radiation (K = 1.5406 Å). Functional groups were analyzed by a Fourier transform infrared spectrometer (FT-IR) (Perkin Elmer Spectrum 100 FT-IR Spectrometer). The IR (infrared) spectrum was recorded in the middle region wavelength of 4000–400 cm^{-1} at a resolution of 4.0 cm^{-1}. A suspension on a Zeta sizer Nano ZS particle analyzer (Malvern) was used to measure the surface charge on the SeNPs. The surface shape and particle elemental analysis were studied using FE-SEM (field emission scanning electron microscope) and HR-TEM (high-resolution transmission electron microscope; Tecnai TM G2 F30) analysis. The DLS (dynamic light scattering) and zeta potential (ZP) analyzer (Malvern Zeta sizer Nano-ZS90, UK) were utilized for measuring the size dimension and surface charge of the synthesized SeNPs.

Mosquito Collection and Culture

Mosquito eggs were collected from stagnant water from a local residential area in Salem, Tamil Nadu, India. The collected eggs were taken to the laboratory and transferred to enamel trays (18 cm L × 13 cm W × 4 cm D) containing 500 mL of water where they were allowed to hatch. The emerged healthy larvae were reared at 29 ± 2°C and 75–85% RH in a 14:10 (L:D) photoperiod fed with a mixture of ground dog biscuits and brewer's yeast at 3:1 ratio. Feeding was stopped when they were grown entirely to pupae, transferred to plastic containers with 500 mL of water for emergence. The container was placed inside a screened cage (90 cm L × 90 cm H × 90 W) to retain emerging adults, for which 10% sucrose in water solution (v/v) was available ad libitum. On day five post-emergence, the adult mosquitoes were provided access to an albino mouse for blood feeding. Glass Petri dishes lined with filter paper containing 50 mL of water were subsequently placed inside the cage for female oviposition mosquitoes.

Molecular Identification

The eggs (F0) were cultured in the laboratory, and the F1 adults obtained from the eggs were used for identification through conventional taxonomy and for developing the DNA barcodes. DNA isolation, polymerase chain reaction (PCR), and cloning were performed [44]. The whole body of a dewinged adult mosquito was homogenized in warm CTAB buffer (Tris 100 mM, EDTA 20 mM, NaCl 1.4 M, CTAB 2%, β-mercaptoethanol 0.2%) and placed in a water bath at 65°C for 1 h. This sample was centrifuged at 9660 g for 10 min at 4°C. The supernatant was discarded and added 24:1 volume of chloroform:isoamyl alcohol mixture. Then, the mixture was shaken vigorously followed by centrifugation at 9660 *g* for 10 min at 4°C. The supernatant was pipetted out and added 0.7 µL of ice-cold isopropanol followed by brief centrifugation. Finally, the DNA pellets settled at the bottom of the Eppendorf tube, and the pellets were washed with 70% ethanol to remove salts. The dried DNA pellet was dissolved in 30–50 µL of sterile RNAse-free distilled water, and finally, the extraction of RNA-free DNA was stored at −80°C until analysis. The universal primers, LCO1490 (5′-GGTCAACAAATC ATAAAGATATTGG-3′) and HCO2198 (5′-TAAACTTCA GGGTGACCAAAAAATCA-3′), were used to amplify the isolated DNA [45]. The amplified PCR product was cloned and used for sequencing. The sequence was submitted to the NCBI sequence database for homology search in GenBank.

Larval Toxicity Assay

Mosquito larvae of F3 laboratory colonies were used for bioassay. Four developmental stages (1st, 2nd, 3rd, and 4th instars) of F3 laboratory-cultured *Ae. aegypti* were treated with three different concentrations (1, 20, and 50 ppm) of biogenic SeNPs, and one sets treated with distilled water without any nanoparticle served as control. Twenty-five actively swimming *Ae. aegypti* immatures of all the above said developmental stages were sieved out from the rearing trays to 250 mL capacity experimental plastic containers containing 100 mL sterile distilled water with selected concentrations of SeNPs and untreated control setup in five replicates [46]. The larvae were fed ad libitum of fine-powdered liver and glucose at a ratio of 3:2 (wt) as an enhanced method of [47] and as described by [48]. The larval mortality was assessed after 24, and 48-h exposure to SeNPs

of known concentrations by probing the larvae with needle and moribund larvae were counted as dead [49]. The control mortalities were corrected by using [50]:

$$\text{Corrected mortality} = {}^{A-B}\!/_{C} * 100$$

$$\text{Percentage mortality} = {}^{X}\!/_{Y} * 100$$

where *A*—observed mortality in treatment, *B*—observed mortality in control, *C*—control mortality, *X*—number of dead larvae, and *Y*—number of larvae introduced.

Histopathological Analysis

Larval tissues from control and treated fourth instar *Ae. aegypti* were dehydrated, fixed in 10% buffered formaldehyde for 24 h, mounted in paraffin blocks and sectioned (8 µm thickness) using a rotary microtome. The fine sections removed without damages were mounted on glass slides and stained with hematoxylin and eosin (HE stain) with melted paraffin for histopathological observation in a bright field light microscope (Model Magnus MLX-B) connected to a computer, and midgut cells of larvae were photographed. The accumulation of tissue damages was observed under a stereomicroscope (Nikon SMZ 1000) and compared with control [51, 52].

Bacterial Inhibition Assay

The growth inhibitory effect of the biogenic SeNPs was evaluated on the bacterial species by the standard disc diffusion method [53]. The pathogenic food bacteria, *S. aureus* (MTCC 96), *E. coli* (MTCC 443), and *S. typhi* (MTCC 98), were procured from Microbial Type Culture Collection and Gene Bank (MTCC), CSIR-Institute of Microbial Technology, Sector 39-A, Chandigarh-160036, India. They were cultured using Agar–agar type I (AA) and Nutrient Broth (NB). Discs of filter paper (6 mm) were soaked with different concentrations (from 25 to 100µL) of SeNPs. The SeNP-impregnated filter paper discs were placed on the bacterial culture plates incubated overnight at 37°C. The diameters of the zones of inhibition (mm) around each filter paper disc were then recorded. The experiments were set up in three replicates.

Molecular Docking Studies

Molecular docking was performed using AutoDock Vina [54] software with AeSCP2 active site due to their in vitro mosquitocidal potencies. Three-dimensional structures of the ligands were downloaded from PubChem [55], and where structures were not available for download, they were sketched, and energy minimized using mmff94 [56] force field. The X-ray crystallographic structure of the AeSCP2 (PDB code: 1PZ4) [57] was retrieved from the Protein Data Bank (PDB) server (www.rcsb.org). Target and ligand preparations were performed with PyRx software, and docking was performed using the Lamarckian Genetic Algorithm (LGA) method. The active site on the protein target was defined by establishing a grid box with the dimensions of X 25.00, Y 20.15, and Z 20.86 Å, with a grid spacing of 0.375 Å, centered on X 24.53, Y 31.15, and Z: 55.0 Å. After completing docking, the best conformation with the lowest docked energy was chosen, and the best pose was saved. For each ligand, ten runs were performed with AutoDock Vina. The interactions of protein–ligand conformations and hydrogen bonds were analyzed using Discovery Studio (Dassault Systèmes BIOVIA, Discovery Studio Modeling Environment, Release 2021, San Diego) and PyMol (PyMOL Molecular Graphics System, Version 1.2r3pre, Schrödinger, LLC).

Statistical Analysis

Probit analysis was used to evaluate the median lethal concentration (LC_{50}) and the respective 95% fiducial limits for each developmental stage of immature *Ae. aegypti*. Mortality data subjected to immature developmental stages were analyzed using analysis of variance (ANOVA) methods, where the 1st, 2nd, 3rd, and 4th instars larvae were dependent variables, and the concentrations used were independent variables. The levels of significance used in all tests were 5%. Tukey's honestly significant difference test assessed the statistical significance of mean differences. Analyses were made using SPSS Software version 16.0.

Results

The F1 adults who emerged from the field-collected eggs grown in the laboratory were used for DNA barcoding. The sequence of the COI gene was searched against the BLAST NR database, which showed 100% similarity and the specimen was confirmed as *Ae. aegypti*. The sequence was submitted in the NCBI gene bank under the accession number (MK882598). The voucher specimen (PU-ZOOMENT-023–2017) is preserved at the Department of Zoology, Periyar University, India. The SeNPs, synthesized by *N. ciliatus* leaf extracts, were preliminarily observed by changing color from orange to red. During the incubation of the blend made up precursor with reduction chemicals, ruby-red appearance was considered a preliminary naked eye technique showing the presence of SeNPs [58]. The ruby-red blend solution was examined under UV–Vis

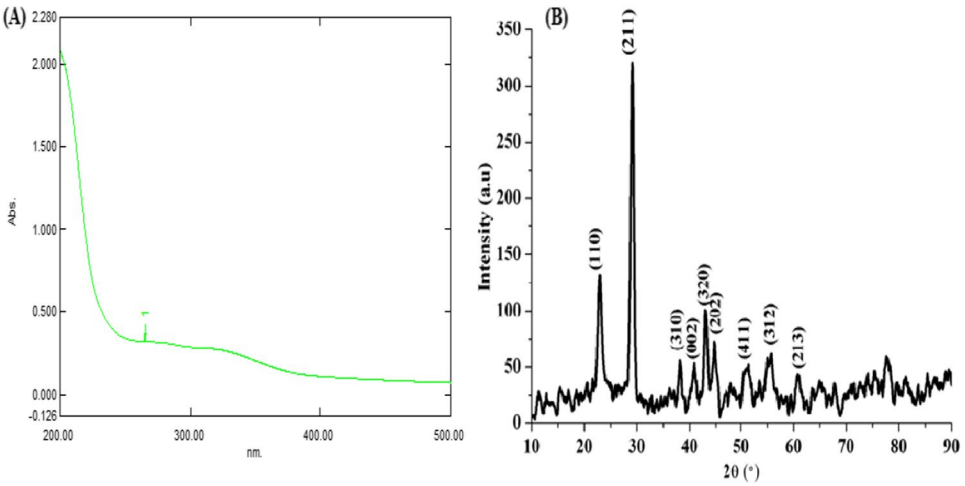

Fig. 1 **A** UV–Vis spectra and **B** XRD analysis of SeNPs synthesized using *N. ciliates* leaf extract

absorption spectroscopy to confirm the absorption band for the formation of SeNPs. The resulting SPR (surface plasmon resonance) band recorded at 265 nm (Fig. 1) confirmed the presence of SeNPs. The ruby-red pellet was freeze-dried to powder form, and it is subjected to XRD analysis. The diffraction of X-rays analysis traveling through the powder from SeNPs mediated by *N. ciliatus* leaf extract was recorded peaks at 32.00°, 41.4°, 68.4°, 62.74°, 61.40°, and 78.05° 2θ corresponding to the facets (110), (211), (310), (002), (320), (202), (411), (312), and (213), signifying the crystalline phase structure of the SeNPs (Fig. 1B). Hence, the XRD pattern has confirmed that the SeNPs formed as a nanocrystalline structure, matching very well with the Joint Committee on Power Diffraction Standard (JCPDS card No. 06–0362) values of selenium powder.

The FT-IR spectra of the SeNPs were analyzed to identify the possible bio-functional molecules responsible for reducing selenious acid to SeNPs and capping the bio-reduced SeNPs. The FT-IR spectrum has recorded major peaks positioned at 3417.31, 2923.13, 2854.19, 2096.12, 1714.09, 1621.05, 1384.64, 1023.26, 668.74, and 468.97 cm^{-1} (Fig. 2).

Moreover, the peaks at 3417.31 cm^{-1} and 1621.05 cm^{-1} assigned for O–H group vibrations of dextran and the C–H stretches in alkanes appear at 2923.13 cm^{-1}. The peak at 2854.19 cm^{-1} appears for C–H stretching vibration. The peaks observed at about 2096.12 cm^{-1} are due to alkene and aromatic = C–H stretching frequency and 1384.64 cm^{-1} (C-H asymmetric bending in CH_2 and CH_3 groups). The peak at around 1714.09 cm^{-1} was attributed to the carboxyl groups. The large and intense band at 1023.26 cm^{-1} represents the superposition of in-plane C-H bending and the characteristic Se-O stretching vibration. Additional bending vibrations of the Se-O bond are emphasized at 668.74 and 468.97 cm^{-1}. From the FT-IR, it could be inferred that the flavonoid, alkaloids, and steroids from leaves served as a potent capping agent on the nanoparticles.

The FE-SEM and HR-TEM images have shown the shape (Fig. 3) of bio-synthesized SeNPs. The morphology of bio-synthesized SeNPs analysis under FE-SEM has revealed an oval shape with agglomeration (Fig. 3A). The HR-TEM image also shows a smooth surface with small agglomeration in two different magnifications (Fig. 3B, C). These images preliminarily represented a particle size of approximately more than 500 nm.

The DLS technique was used to determine the size distribution of biologically synthesized SeNPs (Fig. 4A). The monochromatic laser diffraction collected by the photomultiplier has recorded the red color of the Se colloids. It implied that selenium is either amorphous or monotonic since trigonal selenium ranges from 100 to 1000 nm with a Z-average value of 547.2 nm. Moreover, the distribution of particle size was narrow due to selecting appropriate concentrations of precursors and exposure times using repeated trials. The Zeta sizer's report on the zeta potential of the biologically synthesized SeNPs revealed the stability of the metal nanoparticles in the aqueous medium (Fig. 4B). The zeta potential of the SeNPs mediated through *N. ciliates* leaf extract was −9.16 mV and confirms the strong repulsion among the particles and thereby increases the stability of the nanoparticles.

The selected developmental stages of *Ae. aegypti* (I, II, III, and IV instar) could not withstand the toxicity of biologically synthesized SeNPs even at low dosage. The SeNPs at 50 µg/mL could kill more than 70% of mosquitoes' very early developmental stage at 24 h. The LC_{50} for 1st to 4th developmental instars were 3.71, 14.39, 52.14, and 203.92 µg/mL respectively at 24-h treatment (Table 1). The acquired chi-square values (2.47, 0.624, 0.605, and 0.813 for I, II, III, and IV instars, respectively) prove that the observed mortality is on par with the expected mortality. The mortality rate of *Ae. aegypti* was increased at 48 h of treatment with SeNPs at 1, 20, and 50 µg/mL concentrations (Table 1). About 84% mortality was observed in

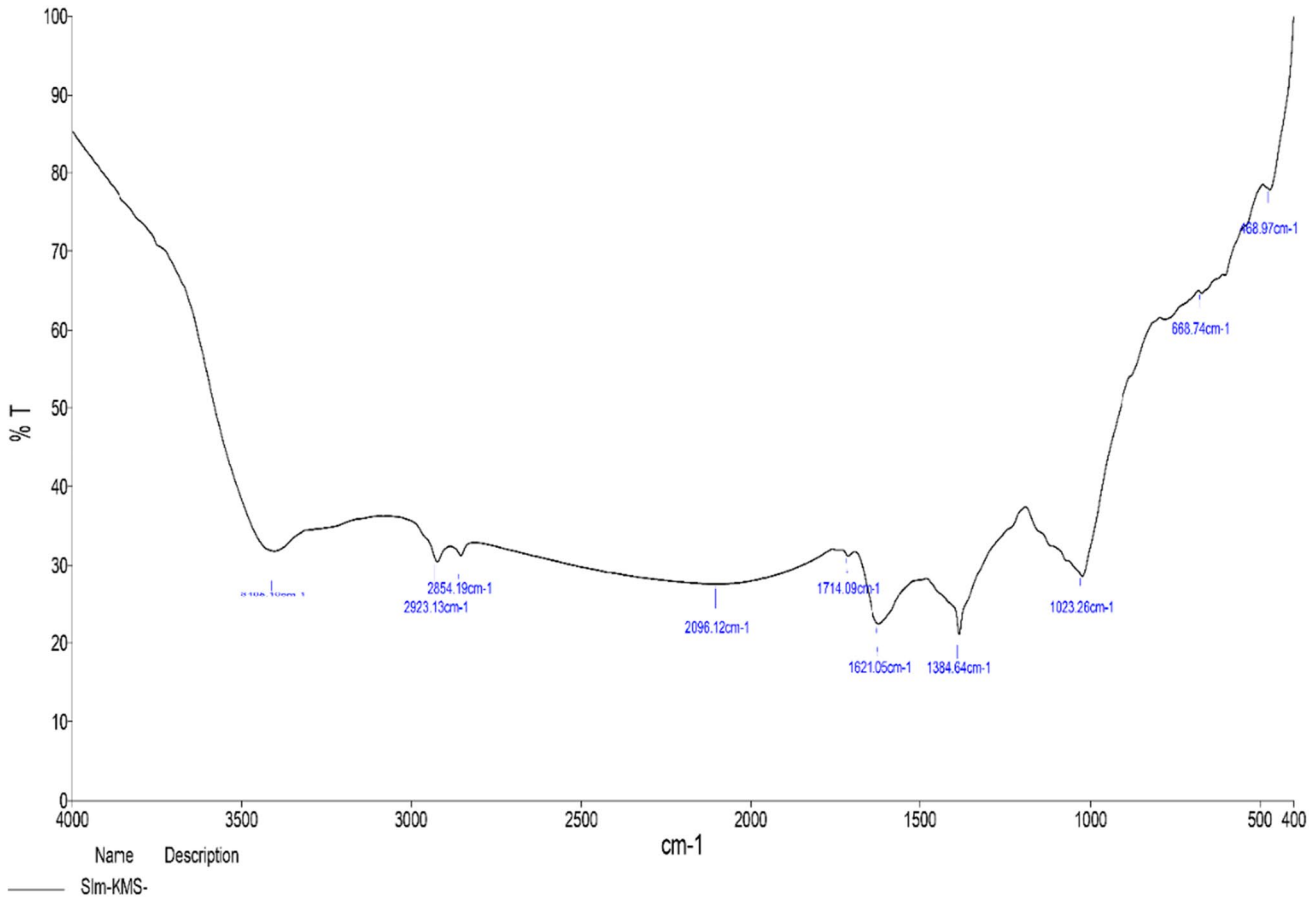

Fig. 2 FT-IR analysis of SeNPs mediated by *N. ciliates* leaf extract

the early developmental stages at treatment with 50 µg/mL concentration. Median lethal concentrations were reduced to 0.916, 2.97, 13.60, and 86.22 µg/mL for 1st to 4th instars respectively at 48-h treatments. The antibacterial activity of SeNPs mediated by *N. ciliates* leaf extract was investigated against the foodborne pathogen, *S. aureus* (MTCC 96), *E. coli* (MTCC 443), and *S. typhi* (MTCC 98) by disc diffusion method and quantitatively assessed based on the zone of inhibition, when treated with 25, 50, 75, and 100 µg/mL concentrations, respectively (Fig. 5).

The exemplary cross-sections of SeNPs treated 4th instar *Ae. aegypti* larva were stained and observed under a light microscope for visualizing the cellular level damage caused by the SeNPs to the insect. The histology of *Ae. aegypti* tissues clearly shows noticeable changes and damages in treated larva compared with the control larva without any damage (Fig. 6A). The larva treated with 1 ppm SeNPs showed microscopically visible damages, including cell lysis, damages in peritrophic membrane, and early stages of epithelial cell rupture (Fig. 6B). The larva treated with 20 ppm SeNPs has shown apparent ruptures in epithelial cells and separated cells (Fig. 6C). The larva treated with 50 ppm SeNPs (Fig. 6D) shows completely disordered and broken epithelial cells, completely broken midgut, caeca, and collapsed larva.

Molecular docking studies were carried to understand the interaction between protein structures and bioactive compounds. The uptake of cholesterol can be reduced by inhibiting AeSCP2 and, in turn, can lead to death in both larval and adult mosquitoes. Hence, for this reason, we intended to target the AeSCP2. For this purpose, potent phytochemical constituents listed in Table 2 that could contribute to the plant's medicinal properties were collected through a literature survey [59] and docked using AutoDock Vina software with AeSCP2 active site.

The phytoconstituents of *N. ciliates* used for the docking study are given in Table 2. Compound β-tocopherol showed the highest affinity with a docking score of −9.3, followed by phytol, 9,12,15-octadecatrienoic acid, methyl ester, and 2-n-heptylcyclopentanone with a docking score of −8.0, −7.9, and −7.2, respectively. The control inhibitor palmitic acid displayed an affinity with a docking score

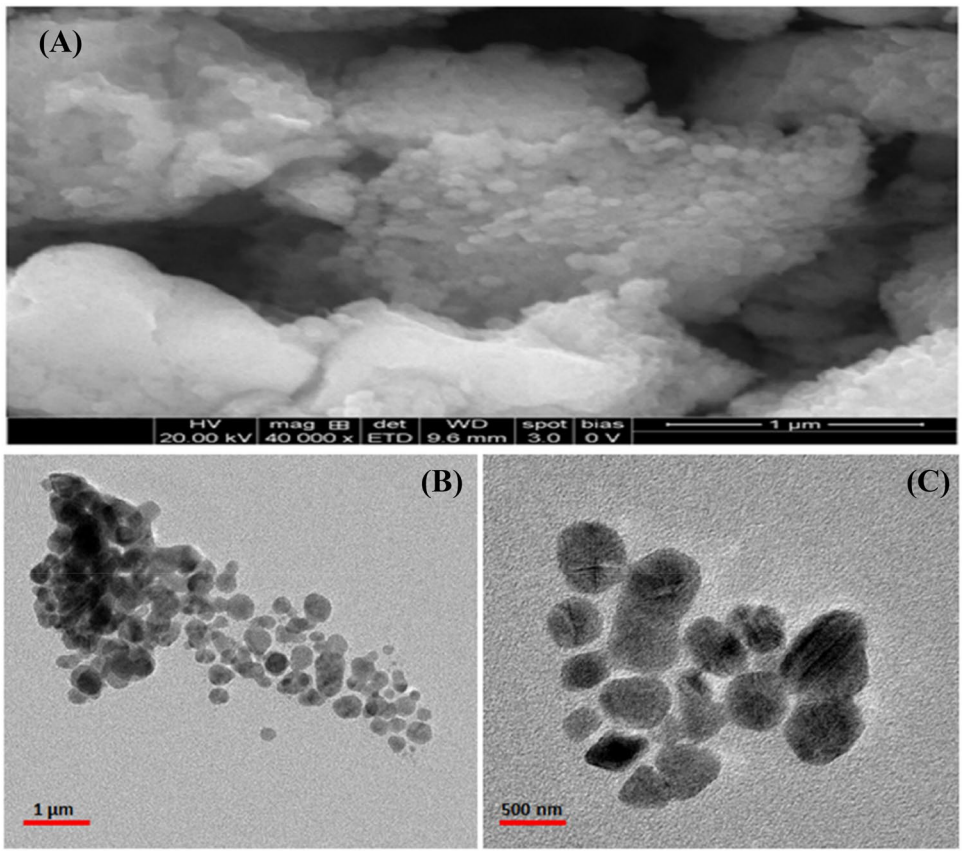

Fig. 3 **A** FE-SEM image (1 µm magnification), and HR-TEM **B**, **C** images (1 µm and 500 nm magnification) of SeNPs synthesized using *N. ciliates* leaf extract

of −6.9. Two other compounds showed a similar docking score to control (−6.9) (Table 3). The docked poses of the top three compounds and the control compounds in the target active site are presented in Fig. 7. The hydrogen bond and pi-pi interactions between the compounds and the target are presented in Fig. 7. The results showed that the compounds had established interactions through hydrogen and pi-pi with the active site residues. The control established a hydrogen bond with the Val26, which could be observed in compounds phytol and 9,12,15-octadecatrienoic acid, methyl ester. Besides establishing conventional interactions, β-tocopherol was found to establish pi-sulfur with the Met71.

Discussion

Mosquitoes control practices are strengthened globally, but there are few challenges, including increasing resistance to insecticides, environmental toxicity, and effects on non-target organisms [60]. Similarly, the control of microbial pathogens is challenging due to the development of resistance [61]. Biogenic nanoparticles are capable of overcoming the challenges and acting more effectively on target species. The biogenic nanoparticles prepared in this investigation show that UV–visible spectral peaks at 265 nm confirm the formation of SeNPs. The UV spectral formation is due to the SPR vibration of SeNPs [62, 63]. A previous study on SeNPs has observed UV–visible spectral peak at 260 nm and reported that it is due to the SPR of the SeNPs [64]. Similarly, the UV–visible absorption spectra of SeNPs were recorded at 261 nm when synthesized using *Diospyros montana* leaf extract [65] and at 270 nm when synthesized using *Emblica officinalis* fruit extract [66]. Further examination has confirmed that the synthesized particles are highly stable, oval SeNP size around 550 nm.

The phytochemicals coated on the surface of the SeNPs are determined using FT-IR by measuring the stretching of bonds within a molecule [67]. The FT-IR spectra of earlier studies on the biogenic synthesis of SeNPs using plant extracts were in concordance with the present study by showing the presence of major and minor peaks assigned to various molecules [68]. An earlier study on the biogenic synthesis of SeNPs using the leaf extract of *Aloe vera* showed that the major and minor peaks were corresponding to the vibrations of molecular bonds that were partially similar to that of the present study [69].

The XRD peaks observed at higher diffraction angles were corresponding to the crystalline planes of SeNPs. Earlier reports on SeNPs synthesized by using the extracts of

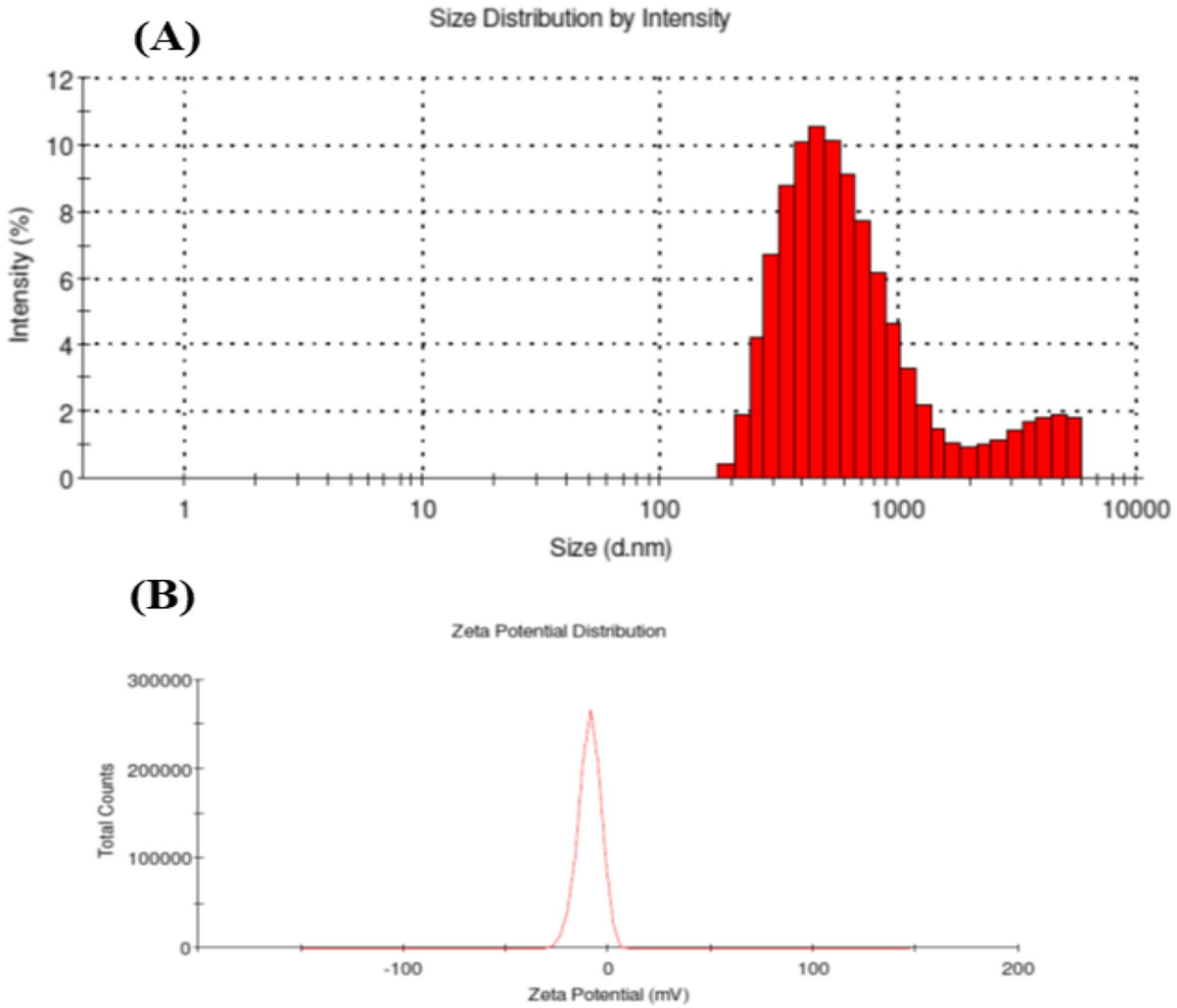

Fig. 4 **A** DLS and **B** zeta potential of SeNPs synthesized using *N. ciliates* leaf extract

Table 1 The larvicidal effect of SeNPs on different larval stages of *Ae. aegypti* at 24- and 48-h observation

Larval stages	Larvae introduced	Mortality/concentration (µg/mL)				LC_{50}	X^2
		Control	1 µg/mL	20 µg/mL	50 µg/mL		
24-h exposure, (%) ± SD							
I instar	100	0 ± 0	$40.00^{d} \pm 4.00$	$58.66^{d} \pm 6.11$	$76.00^{d} \pm 4.00$	3.71	2.47
II instar	100	0 ± 0	$32.00^{c} \pm 4.00$	$49.33^{bc} \pm 6.11$	$61.33^{c} \pm 6.11$	14.39	0.62
III instar	100	0 ± 0	$24.00^{b} \pm 4.00$	$40.00^{b} \pm 4.00$	$52.00^{b} \pm 4.00$	52.14	0.60
IV instar	100	0 ± 0	$12.00^{a} \pm 4.00$	$26.66^{a} \pm 6.11$	$40.00^{a} \pm 4.00$	203.92	0.81
48-h exposure, (%) ± SD							
I instar	100	0 ± 0	$52.00^{d} \pm 4.00$	$69.33^{d} \pm 6.11$	$84.00^{d} \pm 4.00$	0.916	2.30
II instar	100	0 ± 0	$44.00^{c} \pm 4.00$	$57.33^{c} \pm 6.11$	$72.00^{c} \pm 4.00$	2.97	1.88
III instar	100	0 ± 0	$33.33^{b} \pm 6.11$	$48.00^{b} \pm 4.00$	$62.66^{b} \pm 8.32$	13.60	1.47
IV instar	100	0 ± 0	$20.00^{a} \pm 4.00$	$36.00^{a} \pm 4.00$	$48.00^{a} \pm 4.00$	86.22	0.56

Values are mean ± SD of three replicates

SD standard deviation, χ^2 chi-square test

$^{*}p < 0.05$, level of significance

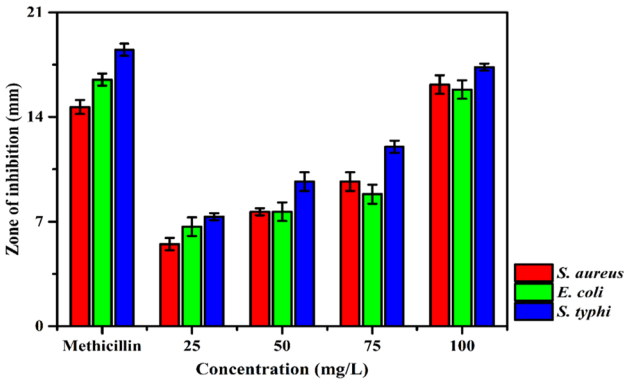

Fig. 5 Food pathogenic antibacterial activity of SeNPs synthesized using *N. ciliates* leaf extract

Theobroma cacao bean shell [70], *Cassia auriculata* leaf [71], and *Spermacoce hispida* aqueous leaf [72] showed similar diffraction peaks corresponding to the crystalline planes of SeNPs. The FE-SEM, HR-TEM images, and DLS report confirmed that the SeNPs synthesized using *N. ciliatus* are spherical-shaped polydispersed particles in a nanoscale ranging between 100 and 1000 nm. Previous studies on the biosynthesis of SeNPs reported that spherical, polydisperse nanoparticles [73, 74] support the present study.

The antiviral and antioxidant activities of SeNPs were reported earlier, and their lower toxicity to non-target organisms has made them one among the medically essential compounds [75, 76]. The mosquitocidal and antibacterial activities were added to the list based on the outcomes of the present study. The toxicity of SeNPs on mosquitoes may be due to ease penetration of the SeNPs into the cells and interaction with the cellular component, leading to the rupture

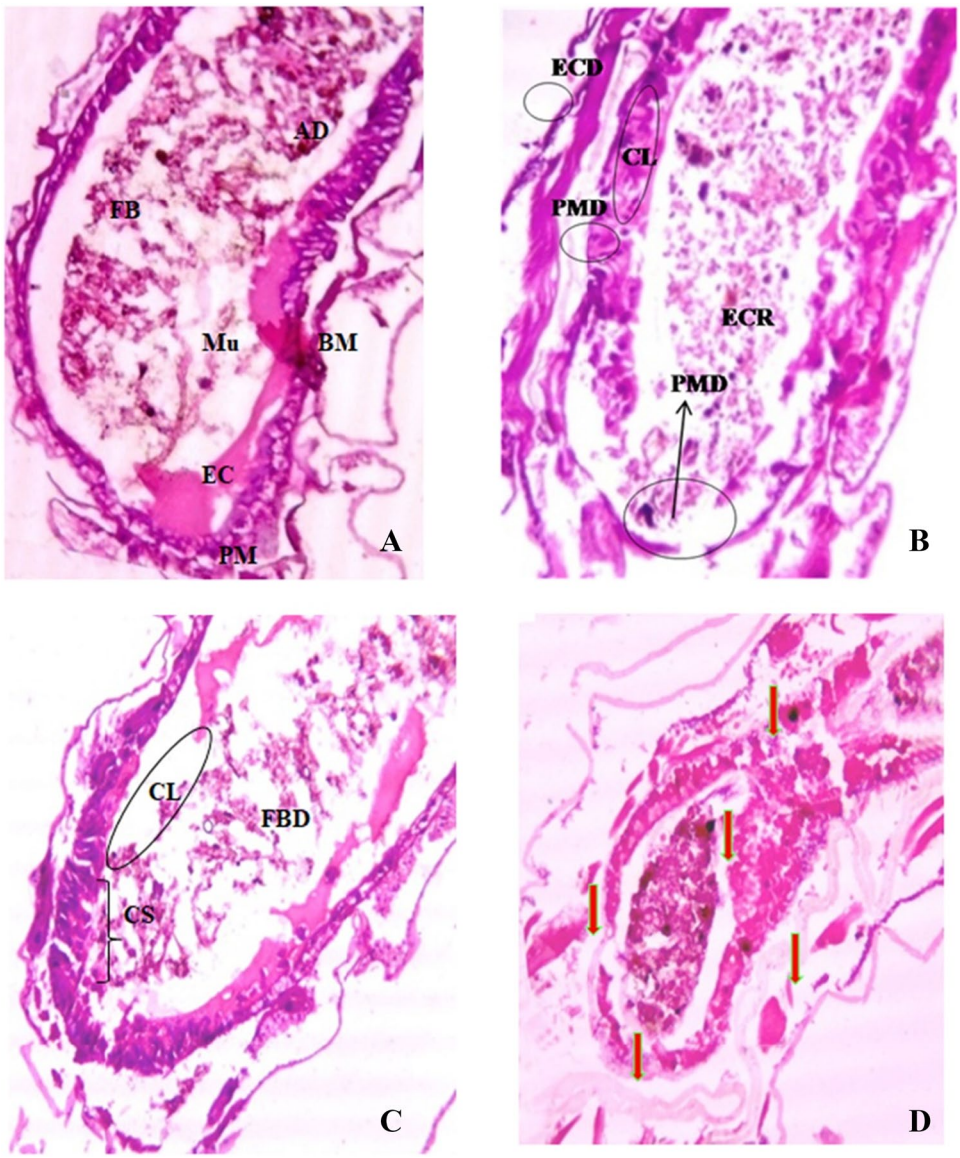

Fig. 6 Histopathological analysis of *Ae. aegypti* larvae treated with SeNPs mediated by *N. ciliates* leaf extract

Table 2 The phytoconstituents of *N. ciliates* used for docking study

Sl. No	Name of the compound	Molecular formula
1	3-Octyne,2,2,7-trimethyl	C11H20
2	Phytol	C20H40O
3	Dibutyl phthalate	C16H22O4
4	(R)-(-)-(Z)-14-Methyl-8-hexadecen-1-ol	C17H34O
5	Hexadecanoic acid, ethyl ester	C18H36O2
6	1-Dodecanol,3,7,11-trimethyl-	C15H32O
7	2-n-Heptylcyclopentanone	C12H22O
8	9,12,15-Octadecatrienoic acid, methyl ester	C19H32O2
9	2-Propenoic acid, 2-(dimethylamino)ethyl ester	C7H13NO2
10	Squalene	C30H50
11	β-Tocopherol	C28H48O2
12	Vitamin E	C29H50O2
13	Campesterol	C28H48O
14	Stigmasterol	C29H48O
15	β-Amyrin	C30H50O

of the tissues and cellular components, as shown in the histopathological analysis (Fig. 6). The exact complex interactions of SeNPs on the molecular components are yet to be delineated. The preparation of nanoparticles with bioactive principles increases its toxicity on mosquitoes [77]. The biologically active SeNPs are capable of denaturing sulfur-containing proteins or phosphorous-containing compounds like DNA. Thus, it reduces the cellular membrane permeability and reduces ATP synthesis, which finally causes the loss of cellular function and cell death [78].

In the present study, the immature developmental stages of *Ae. aegypti* were susceptible to SeNPs at very low dosage, providing a median lethal concentration of 86.22 µg/mL for the fourth instar larvae. An earlier study on SeNPs shows that the larvicidal activity on *Ae. aegypti* with a median lethal concentration of 104.13 mg/L for the fourth instar larvae [79] was far behind the toxicity level with the present study. This may be due to the way of preparation providing us with a more stable and active nanoparticle. The method of preparation and plant material used as reducing and capping agents could also change the toxicity level of the nanoparticles synthesized using them. Size and shape play a significant role in the toxicity behavior of nanomaterial [80].

Table 3 The binding energy of phytoconstituents from *N. ciliates* showing above the control compound

Ligand	Binding energy
β-Tocopherol	−9.3
Phytol	−8
9,12,15-Octadecatrienoic acid, methyl ester	−7.9
2-n-Heptylcyclopentanone	−7.2
1-Dodecanol,3,7,11-trimethyl-	−6.9
(R)-(-)-(Z)-14-Methyl-8-hexadecen-1-ol	−6.9
Palimitic acid (control)	−6.9

As conventional mosquito control was carried out using insecticides of chemical origin, contaminating the environment was inevitable. This requires alternate eco-friendly approaches for controlling the vector mosquitoes at the larval stage. During cholesterol conversion/uptake carried out in *Ae. aegypti* in the presence of the carrier protein AeSCP-2, search for AeSCP-2-specific inhibitors from natural origin seems essential. The SCP-2 contains a sterol-binding domain (SCP-2 domain). Though found in vertebrates, the mosquito AeSCP-2 seems unique due to its non-peroxisomal and low-molecular-weight protein characters in the SCP-2 gene family [81, 82]. The homolog of AeSCP-2 is found in the genome of *Anopheles gambiae*, having > 85% similarity [83, 84], which indicates a highly conserved nature of mosquito SCP-2 proteins between the two species. As phytochemical constituents from *N. ciliatus* show comparable and better interactions of palmitic acid, these could be exploited as alternative pesticides for targeting *Ae. aegypti*.

The antimicrobial activity of SeNPs was confirmed in previous work done by [85]. In this study, SeNPs developed inhibitory zones and proved their capability to kill bacterial cells at 25 µg/mL concentration. Similar results on SeNPs posing bacterial inhibition at a low concentration ranging close to 25 µg/mL was reported by preceding researchers [86, 87]. Effective toxicity of the SeNPs may be due to the energy less penetration of the particles into the *S. aureus* bacteria by chemisorption, where the lipoproteins involved are of the diacyl and triacyl forms [88]. A recent study reported that the nanoparticles are excellent barriers preventing the entry of foodborne pathogens for a long time when incorporated with the food processing and food package materials [89]. The foodborne pathogens exhibit

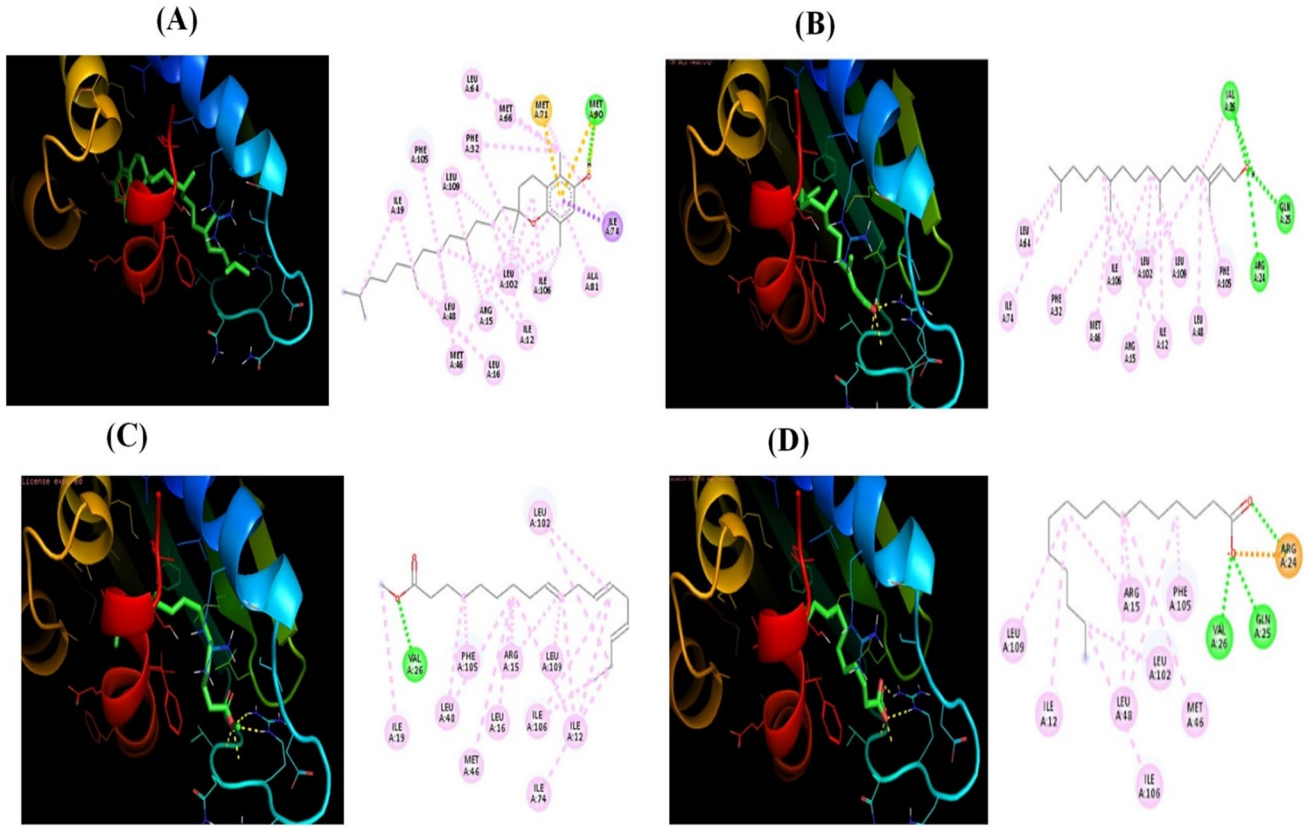

Fig. 7 Ligand poses of compounds in the active site of AeSCP2. **A** β-Tocopherol. **B** Phytol. **C** 2-n-Heptylcyclopentanone. **D** Palmitic acid (control). Yellow dashes indicate hydrogen bonding

their exacerbating activity by the formation of biofilm. The SeNPs are an excellent anti-biofilm agent that suppresses the severity of the infection of a foodborne pathogen [90]. The foodborne pathogens are generally lyzed or killed by the production of reactive oxygen species (ROS) on the surface of the nanoparticles when it penetrates the bacterial cell wall and happens to hit with photons or other reactive agents [91]. Another possible reason could be the interaction of nanoparticles with the thiol groups present in the protein leading to the destruction of the cell wall of the foodborne pathogens [92].

Conclusion

Pesticides and drugs that are in use today should be environmentally safe and economically viable. Hence, while designing pesticides, the above facts must be taken into account. SeNPs are naturally a trace element required by the human body. Furthermore, the biogenic procedure and biocoating of the SeNPs by active metabolites of *N. ciliatus* make it much safer and most viable. The eco-friendly SeNPs was showed a significant effect on the dengue vector, *Ae. aegypti*. The histopathological examination revealed internal damages caused by the SeNPs in *Ae. aegypti*. The *N. ciliates*-mediated SeNPs also exhibited growth inhibitory performance against the pathogenic bacteria, *S. aureus* (MTCC 96), *E. coli* (MTCC 443), and *S. typhi* (MTCC 98). *In silico* molecular docking study revealed the mechanistic action of the phytoconstituents of *N. ciliatus* on *Ae. aegypti*. Since the production of nanoparticles follows through a green route, they are non-hazardous to the environment and other animals. Future studies must be conducted to evaluate the mechanism of SeNPs in antibacterial activity.

Acknowledgements The authors sincerely acknowledge and thank Periyar University, Salem, Tamil Nadu, for providing all required laboratory facilities to conduct this research work.

Author Contribution Krishnan Meenambigai: data curation, methodology, writing – original draft; Ranganathan Kokila: methodology, formal analysis; Kandasamy Chandhirasekar: data curation, formal analysis; Ayyavu Thendralmanikandan: methodology; Durairaj Kaliannan: data curation, formal analysis; Kalibulla Syed Ibrahim: formal analysis, resources, bioinformatics; Shobana Kumar: data curation, formal analysis; Wenchao Liu: data curation, validation, writing – review and editing; Balamuralikrishnan Balasubramanian: conceptualization,

writing – review and editing; Arjunan Nareshkumar: conceptualization, supervision, validation, visualization, writing – review and editing.

Funding Authors are thankful to the University Grants Commission (UGC), New Delhi, India, for the award of Rajiv Gandhi National Fellowship with financial support (Ref No: F1-17.1/ 2015–16/ RGNF2015-17 –SC-TAM-10313) to carry out this research work.

Data Availability Not applicable.

Code Availability Not applicable.

Declarations

Ethics Approval and Consent to Participate Not applicable.

Consent for Publication Not applicable.

Conflict of Interest The authors declare no competing interests.

References

1. Benelli G, Mehlhorn H (2016) Declining malaria, rising of dengue and Zika virus: insights for mosquito vector control. Parasitol Res 115:1747–1754. https://doi.org/10.1007/s00436-016-4971-z
2. Dinesh D, Murugan K, Madhiyazhagan P, Panneerselvam C, MaheshKumar P, Nicoletti M, Jiang W, Benelli G, Chandramohan B, Suresh U (2015) Mosquitocidal antibacterial activity of green-synthesized silver nanoparticles from *Aloe vera* extracts: towards an effective tool against the malaria vector *Anopheles stephensi*? Parasitol Res 114:1519–1529. https://doi.org/10.1007/s00436-015-4336-z
3. Karin L, Carina Z, Katja S, Adelheid O, Dominik B, Katharina B, Melanie W, Beate P, Hans PF, Franz R (2015) Mosquitoes (Diptera: Culicidae) and their relevance as disease vectors in the city of Vienna Austria. Parasitol Res 114:707–713. https://doi.org/10.1007/s00436-014-4237-6
4. Mehlhorn H, Al-Rasheid KA, Al-Quraishy S, Abdel-Ghaffar F (2012) Research and increase of expertise in arachno-entomology are urgently needed. Parasitol Res 110:259–265. https://doi.org/10.1007/s00436-011-2480-7
5. Murugan K, Panneerselvam C, Subramaniam J, Madhiyazhagan P, Hwang JS, Lan W, Dinesh D, Suresh U, Roni M, Higuchi A, Nicoletti M, Benelli G (2016) Eco-friendly drugs from the marine environment: sponge weed-synthesized silver nanoparticles are highly effective on *Plasmodium falciparum* and its vector *Anopheles stephensi,* with little non-target effects on predatory copepods. Environ Sci Pollut Res 23:16671–16685. https://doi.org/10.1007/s11356-016-6832-9
6. WHO, 2017, Dengue and dengue haemorrhagic fever - fact sheet no 117, Available at, http://www.who.int/mediacentre/factsheets/fs117/en/.2017. Accessed 7 Jan
7. Tome HV, Pascini TV, Dangelo RA, Guedes RN, Martins GF (2014) Survival and swimming behavior of insecticide-exposed larvae and pupae of the yellow fever mosquito *Aedesaegypti*. Parasit Vectors 7:1–9. https://doi.org/10.1186/1756-3305-7-195
8. P.V. Gonzalez, L. Harburguer, P.A. Gonzalez-Audino, H.M. Masuh, The use of *Aedesaegypti* larvae attractants to enhance the effectiveness of larvicides, Parasitol Res 115 (2016) 2185–2190. https://doi.org/10.1007/s00436-016-4960-2
9. B. Morejon, F. Pilaquinga, F. Domenech, D. Ganchala, A. Debut, M. Neira (2018) Larvicidal activity of silver nanoparticles synthesized using extracts of *Ambrosia arborescens* (Asteraceae) to Control *Aedesaegypti*L. (Diptera: Culicidae), J Nanotechnol 2018. https://doi.org/10.1155/2018/6917938
10. P.B. Patil, K.J.Gorman, S.K. Dasgupta, K.V. Seshu Reddy, S.R. Barwale U.B. Zehr (2018) Self-limiting OX513A *Aedesaegypti*demonstrate full susceptibility to currently used insecticidal chemistries as compared to Indian wild-type *Aedesaegypti*, Hindawi Psyche 2018. https://doi.org/10.1155/2018/781464
11. Govindarajan M, Benelli G (2016) α-Humulene and β-elemene from Syzygiumzeylanicum(Myrtaceae) essential oil: highly effective and eco-friendly larvicidesagainsAnophelessubpictus, Aedesalbopictus, and Culextritaeniorhynchus(Diptera:Culicidae). Parasitol Res 115:2771–2778. https://doi.org/10.1007/s00436-016-5025-2
12. Mishra R, Bohra A, Kamaal N, Kumar K, Gandhi K, Sujayan GK, Saabale PR, SatheeshNaik SJ, Sarma BK, Dharmendra K, Mishra M, Srivastava DK, Narendra PS (2018) Utilization of biopesticides as sustainable solutions for management of pests in legume crops: achievements and prospects. Egypt J Biol Pest Co 28:1–11. https://doi.org/10.1186/s41938-017-0004-1
13 Soni N, Prakash S (2014) Silver nanoparticles: a possibility for malarial and filarial vector control technology. Parasito Res 113(11):4015–4022. https://doi.org/10.1007/s00436-014-4069-4
14 Amita H, Snehali D, Naba Kumar M (2016) Mosquito larvicidal activity of cadmium nanoparticles synthesized from petal extracts of marigold (Tagetes sp.) and rose (Rosa sp.) flower. J Parasit. 40(4):1519–1527. https://doi.org/10.1007/s12639-015-0719-4
15. M. Yazhiniprabha, B. Vaseeharan, *In vitro* and *in vivo* toxicity assessment of selenium nanoparticles with significant larvicidal and bacteriostatic properties. Mater Sci Eng C 109763 (2019). https://doi.org/10.1016/j.msec.2019.109763.
16. Li T, Lan Q, Liu N (2009) Larvicidal activity of mosquito sterol carrier protein-2 inhibitors to the insecticide-resistant mosquito *Culexquinquefasciatus*(Diptera: Culicidae). J Med Entomol 46:1430–1435. https://doi.org/10.1603/033.046.0626
17. H. Ma, Y. Ma, X. Liu, D. H. Dyer, P. Xu, K. Liu, Q. Lan, H. Hong (2015) JianxinPeng R. Peng, NMR structure and function of *Helicoverpaarmigera*sterol carrier protein-2, an important insecticidal target from the cotton bollworm. Sci Rep 5:1–14. https://doi.org/10.1038/srep18186.
18. Dyer DH, Vyazunova I, Lorch JM, Forest KT, Lan Q (2009) Characterization of the yellow fever mosquito sterol carrier protein-2 like 3 gene and ligand-bound protein structure. Mol Cell Biochem 326:67–77. https://doi.org/10.1007/s11010-008-0007-z
19. Radek JT, Dyer DH, Lan Q (2010) Effects of mutations in *Aedesaegypti*sterol carrier protein-2 on the biological function of the protein. Biochemistry 49:7532–7541. https://doi.org/10.1021/bi902026v
20. Kim MS, Wessely V, Lan Q (2005) Identification of mosquito sterol carrier protein-2 inhibitors. J Lipid Res 46:650–657. https://doi.org/10.1194/jlr.M400389-JLR200
21. Kumar RB, Shanmugapriya B, Thiyagesan K, Kumar SR, Xavier SM (2010) A search for mosquito larvicidal compounds by blocking the sterol carrying protein, AeSCP-2, through computational screening and docking strategies. Pharmacognosy Res 2:247–253. https://doi.org/10.4103/0974-8490.69126
22. Singarapu KK, Ahuja A, Potula PR, Ummanni R (2016) Solution nuclear magnetic resonance studies of sterol carrier protein 2 like 2 (SCP2L2) reveal the insecticide specific structural characteristics of SCP2 proteins in *Aedesaegypti*mosquitoes. Biochemistry 55:4919–4927. https://doi.org/10.1021/acs.biochem.6b00322
23. Bintsis T (2017) Foodborne pathogens. AIMS Microbiol 3:529–563. https://doi.org/10.3934/microbiol.2017.3.529

24. Yang S, Xiuguo H, Ying Y, Han Q, Zhifeng Y, Yang L, Jing W, Tingting T (2018) Bacteria-Targeting nanoparticles with microenvironment-responsive antibiotic release to eliminate intracellular *Staphylococcus aureus* and associated infection. ACS Appl Mater Interfaces 10:14299–14311. https://doi.org/10.1021/acsami.7b15678
25. Joseph F, Thomas R, Webster J (2012) Cytotoxicity of selenium nanoparticles in rat dermal fibroblasts. Int J Nanomedicine 7:3907–3914. https://doi.org/10.2147/IJN.S33767
26. WHO, 2014, Initiative to estimate the global burden of foodborne diseases: information and publications. Geneva: World Health Organ 2014.
27. N. Amajoud, A. Leclercq, M. Soriano, H. Bracq-Dieye, M. El Maadoudi, N.S. Senhaji (2018) Prevalence of *Listeria spp*. and characterization of *Listeria monocytogenes* isolated from food products in Tetouan Morocco. Food Control 84:436–441. https://doi.org/10.1016/j.foodcont.2017.08.023.
28. Tsiraki MI, Yehia HM, Elobeid T, Osaili T, Sakkas H, Savvaidis IN (2018) Viability of and Escherichia coli O157:H7 and Listeria monocytogenesin a delicatessen appetizer (yogurt-based) salad as affected by citrus extract (Citrox©) and storage. Food Microbiol 69:11–17. https://doi.org/10.1016/j.fm.2017.07.014
29. C. Shi, X. Zhang, X. Zhao, R. Meng, Z. Liu, X. Chen, Na, G. Synergistic interactions of nisin in combination with cinnamaldehyde against *Staphylococcus aureus* in pasteurized milk. Food Control 71, (2017) 10–16. https://doi.org/10.1016/j.foodcont. 2016.06.020
30. A.A. Alfuraydi, S.M. Devanesan, M. Al-Ansari, M.S. AlSalhi, A.J. Ranjitsingh, Eco-friendly green synthesis of silver nanoparticles from the sesame oil cake and its potential anticancerandantimicrobialactivities. J Photochem Photobiol B 192 (2019)83–89. https://doi.org/10.1016/j.jphotobiol.2019.01.011
31. Oktar FN, Yetmez M, Ficai D, Ficai A, Dumitru F, Pica A (2015) Molecular mechanism and targets of the antimicrobial activity of metal nanoparticles. Curr Top Med Chem 15:1583–1588. https://doi.org/10.2174/1568026615666150414141601
32. Iavicoli I, Leso V, Schulte PA (2016) Biomarkers of susceptibility: state of the art and implications for occupational exposure to engineered nanomaterials. Toxicol Appl Pharmacol 299:112–124. https://doi.org/10.1016/j.taap.2015.12.018
33. Shakibaie M, Khorramizadeh MR, Faramarzi MR (2010) Biosynthesis and recovery of selenium nanoparticles and the effects on matrix metalloproteinase-2 expression. Biotech Appl Bioche 56:7–15. https://doi.org/10.1042/BA20100042
34. Xiao N, Lou MD, Lu YT, Yang LL, Liu Q, Liu B (2017) Ginsenoside Rg5 attenuates hepatic glucagon response via suppression of succinate-associated HIF-1α induction in HFD-fedmice. Diabetologia 60:1084–1093. https://doi.org/10.1007/s00125-017-4238-y
35. C. Vetrivel, K. Durairaj, D. Kalaimurugan, M. Viji, E. Murugesh, L. Wen Chao, B. Balamuralikrishnan, A. Maruthupandia Green synthesis of selenium nanoparticles mediated from *Ceropegia bulbosa Roxb* extract and its cytotoxicity, antimicrobial, mosquitocidal and photocatalytic activities. Sci Rep 11 (2021) 1032. https://doi.org/10.1038/s41598-020-80327-9
36. Meenambigai K, Kokila R, Premkumar M, Pazhanivel T, Sivashanmugan K, Nareshkumar A (2020) Leaf extract of *Dillenia indica* as a source of selenium nanoparticles with larvicidal and antimicrobial potential toward vector mosquitoes and pathogenic microbes. Coatings 10:626. https://doi.org/10.3390/coatings10070626
37. Venkatesan A, Sujatha V (2019) Green synthesis of selenium nanoparticle using leaves extract of *Withania somnifera* and its biological applications and photocatalytic activities. BioNanoScience 9:105–116. https://doi.org/10.1007/s12668-018-0566-8
38. Subarani S, Sabhanayakam S, Kamaraj C (2013) Studies on the impact of biosynthesized silver nanoparticles (AgNPs) in relation to malaria and filariasis vector control against *Anopheles stephensi Liston* and *Culexquinquefasciatus Say* (Diptera: Culicidae). Parasitol Res 112:487–499. https://doi.org/10.1007/s00436-012-3158-5
39. Rameshkumar R, Largia MJV, Satish L, Shilpha J, Ramesh M (2017) In vitro mass propagation and conservation of *Nilgirianthusciliatus* through nodal explants: a globally endangered, high trade medicinal plant of Western Ghats. Plant Biosys Int J Plant Biol 151:204–211. https://doi.org/10.1080/11263504.2016.1149120
40. George M, Joseph L, Sony S (2017) Evaluation of analgesic activity of ethanolic extract of Strobilanthes ciliates Nees. J Pharm Innov 6:326–328
41. Neethu V, SheronSheeba J, Jasmine TS, Divya GS (2014) Study of phytochemical and antimicrobial potential of the leaves of *Nilgirianthusciliatus* Linn. Int J Appl Biol Pharm 5:150–152
42. Reneela P, Shubashini K (2010) Triterpenoid and sterol constituents of *Strobilanthes ciliatus*Nees. Indian J Nat Prod 6:35–38
43. D.J. Tan, H. Dvinge, A. Christoforou, P. Bertone, A. Martinez Arias, K.S. Lilley, Mapping organelle proteins and protein complexes in *Drosophilamelanogaster*. J Proteome Res 8 (2009) 2667–2678.https://doi.org/10.1021/pr800866n.
44. Ramasubramanian T, Ramaraju K, Pandey SK (2015) DNA barcodes of sugarcane Aleyrodids. Int Sugar J 117:206–211
45. Fang C, Zhong H, Lin Y, Chen B, Han M, Ren H, Lu H, Jacob M, Luber M, Xia M, Li W, Stein S, Xu X, Zhang W, Drmanac R, Wang J, Yang H, Hammarstrom L, Aleksandar D, Kostic K, Li J (2018) Assessment of the cPAS-basedBGISEQ-500platform for meta genomic sequencing. Giga Sci 7:1–8. https://doi.org/10.1093/gigascience/gix133
46. WHO, (2005) Guidelines for laboratory and field testing of mosquito larvicides.Communicable disease control, prevention and eradication, WHO pesticide evaluation scheme. WHO Geneva WHO/CDS/WHOPES/GCDPP/1.3. 2005.
47. Roberts N (1998) Holocene book reviews on second editions. The Holocene London 8:751–754. https://doi.org/10.1191/095968398669623867
48. Nareshkumar A, Jeyalalitha T, Murugan K, Madhiyazhagan P (2013) Bioefficacy of plant mediated gold nanoparticles and *Anthocepholuscadamba* on filarial vector, *Culexquinquefasciatus*(Insecta: Diptera: Culicidae). Parasitol Res 112:1053–1063. https://doi.org/10.1007/s00436-012-3232-z
49. Azmi W, Sani RK, Banerjee UC (1998) Biodegradation of triphenylmethane dyes. Enzyme Microb Technol 22:185–191. https://doi.org/10.1016/S0141-0229(97)00159-2
50. Abbott WS (1925) A method of computing the effectiveness of an insecticide. J Econ Entomol 18:265–267
51. Sahar F (2010) Histopathological effects of Fenugreek (Trigonellafoenumgraceum) extracts on the larvae of the mosquito Culexquinquefasciatus. J Arab Soc Med Res 5:123–130
52. Fallatah SA, Khater EI (2010) Potential of medicinal plants in mosquito control. J Egypt Soc Parasitol 40:1–26
53. Diao WR, Hu QP, Feng SS, Li WQ, Xu JG (2013) Chemical composition and antibacterial activity of the essential oil from green huajiao (*Zanthoxylumschinifolium*) against selected foodborne pathogens. J Agric Food Chem. 61:6044–6049. https://doi.org/10.1021/jf4007856
54. Trott O, Olson AJ (2010) AutoDockVina: improving the speed and accuracy of docking with a new scoring function, efficient optimization and multithreading. J Comput Chem 31:455–461. https://doi.org/10.1002/jcc.21334
55. Kim S, Cheng J, Gindulyte T, Li AJQ, Shoemaker BA, Thiessen PA, Yu B, Zaslavsky L, Zhang J, Bolton EE, PubChem in, (2021) new data content and improved web interfaces. Nucleic acids Res 49(2019):D1388–D1395. https://doi.org/10.1093/nar/gkaa971

56. T.A. Halgren, Merck molecular force field. I. Basis, form, scope, parameterization, and performance of *MMFF94,* J. Comput. Chem. 17 (1996) 490–519. https://doi.org/10.1002/(SICI)1096-987X(199604)17:5/6<490::AID-JCC1>3.0.CO;2-P.
57 Dyer DH, Lovell S, Thoden JB, Holden HM, Rayment I, Lan Q (2003) The structural determination of an insect sterol carrier protein-2 with a ligand-bound C16 fatty acid at 1.35-Å resolution. J Biol Chem 278:39085–39091. https://doi.org/10.1074/jbc.m306214200
58. Ramamurthy CH, Sampath KS, Arunkumar P, SureshKumar M, Sujatha V, Premkumar K, Thirunavukkarasu C (2013) Green synthesis and characterization of selenium nanoparticles and its augmented cytotoxicity with doxorubicin on cancer cells. Bioprocess Biosyst Eng 36:1131–1139. https://doi.org/10.1007/s00449-012-0867-1
59. Srinivasan M, Padmaja B, Sudharsan N (2013) Phytochemical identification of *Nilgirianthusciliatus*by GC-MS analysis and its DNA protective effect in cultured lymphocytes. Asian J Biomed Pharm Sci 3:14–17
60. Benelli G, Iacono AL, Canale A, Mehlhorn H (2016) Mosquito vectors and the spread of cancer:an over looked connection? Parasitol Res 115:2131–2137. https://doi.org/10.1007/s00436-016-5037-y
61. Li B, Webster TJ (2018) Bacteria antibiotic resistance: new challenges and opportunities for implant-associated orthopaedic infections. J Orthop Res 36:22–32. https://doi.org/10.1002/jor.23656
62. Mishra RR, Prajapati S, Das J, Dangar TK, Das N, Thatoi H (2018) Reduction of selenite to red elemental selenium by moderately halo tolerant*Bacillus megaterium*strains isolated from Bhitarkanika mangrove soil and characterization of reduced product. Chemosphere 84:1231–1237. https://doi.org/10.1016/j.chemosphere.2011.05.025
63. Yang LB, Shen YH, Xie AJ, Liang JJ, Zhang BC (2008) Synthesis of Se nanoparticles by using TSA ion and its photocatalytic application for decolorization of congo red under UV irradiation. Mater Res Bull 43:572–582. https://doi.org/10.1016/j.materresbull.2007.04.012
64. Anu K, Singaravelu G, Murugan K, Benelli G (2017) Green-synthesis of selenium nanoparticles using garlic cloves (*Allium sativum*): biophysical characterization and cytotoxicity on vero cells. J Clust Sci 28:551–563. https://doi.org/10.1007/s10876-016-1123-7
65. Kokila K, Elavarasan N, Sujatha V (2017) *Diospyrosmontana* leaf extract-mediated synthesis of selenium nanoparticles and its biological applications. New J Chem 41:7481–7490. https://doi.org/10.1039/C7NJ01124E
66. Gunti L, Dass RS, Kalagatur NK (2019) Phytofabrication of selenium nanoparticles from *Emblicaofficinalis* fruit extract and exploring its biopotential applications: antioxidant, antimicrobial, and biocompatibility. Front Microbiol 10:1–17. https://doi.org/10.3389/fmicb.2019.00931
67. Movasaghi Z, Rehman DI (2008) Fourier transform infrared (FTIR) spectroscopy of biological tissues. Appl Spectrosc Rev 43:134–179. https://doi.org/10.1080/05704920701829043
68. J. Vyas S. Rana, Synthesis of selenium nanoparticles using *Allium sativum* extract and analysis of their antimicrobial property against gram positive bacteria. J Pharm Innov 7 (2018) 262–266.https://doi.org/10.21276/ijpbs.2019.9.1.46.
69. B. Fardsadegh, H. Jafarizadeh- Malmiri, *Aloe vera* leaf extract mediated greensynthesis of selenium nanoparticles and assessment of their in vitro antimicrobial activity against spoilage fungi and pathogenic bacteria strains, Green Process. Synth.8 (2019) 399–407. https://doi.org/10.1515/gps-2019-0007.
70. Mellinas C, Jimenez A, Maria D, Garrigos C (2019) Microwave-assisted green synthesis and antioxidant activity of selenium nanoparticles using *Theobroma cacao* L bean shell extract. Molecules 24:40–48. https://doi.org/10.3390/molecules24224048
71. Anushia C, Sampathkumar P, Ramkumar L (2009) Antibacterial and antioxidant activities in *Cassia auriculata*. Glob J Pharmacol 3:127–130
72. Vennila K, Chitra L, Balagurunathan R, Palvannan T (2018) Comparison of biological activities of selenium and silver nanoparticles attached with bioactive phytoconstituents: green synthesized using Spermacoce hispida extract. Adv Nat Sci Nanosci Nanotechnol 9:015005. https://doi.org/10.1088/2043-6254/aa9f4d
73. P. Sribenjarat, N. Jirakanjanakit, K. Jirasripongpun, Selenium nanoparticles biosynthesized by garlic extract as antimicrobial agent. Sci Eng Health Stud 14 (2020) 22–31. https://doi.org/10.14456/sehs.2020.3
74. R.S.R. Radhika, S. Gayathri, Extracelluar biosynthesis of selenium nanoparticles using some species of *Lactobacillus*. Indian J Geo-Mar Sci 44 (2015) 766–775. http:// hdl.handle.net/123456789/34805.
75. Beheshti N, Soflaei S, Shakibaie M, Yazdi MH, Ghaffarifar F, Dalimi A (2013) Efficacy of biogenic selenium nanoparticles against Leishmania major: in vitro and in vivo studies. J Trace Elem Med Biol 27:203–207. https://doi.org/10.1016/j.jtemb.2012.11.002
76. M. Shakibaie, A.R. Shahverdi, M.A. Faramarzi, G.R. Hassanzadeh, H.R. Rahimi, O. Sabzevari, Acute and subacute toxicity of novel biogenic selenium nanoparticles in mice. Pharm Biol 51 (2013) 58–63.https://doi.org/10.3109/13880209.2012.710241
77. Muthukumaran U, Govindarajan M, Rajeswary M (2015) Green synthesis of silver nanoparticles from *CassiaroxBurghii*: a most potent power for mosquito control. Parasitol Res 114:4385–4395. https://doi.org/10.1007/s00436-015-4677-7
78 Shankar SS, Rai A, Ankamwar B, Singh A, Ahmad A, Sastry M (2004) Biological synthesis of triangular gold nanoprisms. Nature Mater 3:482–488. https://doi.org/10.1038/nmat1152
79. Sowndarya P, Ramkumar G, Shivakumar MS (2017) Green synthesis of selenium nanoparticles conjugated *Clausenadentata* plant leaf extract and their insecticidal potential against mosquito vectors. Artif Cells Nanomed Biotechnol. 45:1490–1495. https://doi.org/10.1080/21691401.2016.1252383
80. Saura SC, Hayes AW (2017) Toxicity of nanomaterials found in human environment: a literature review. Toxicol Res Appl 1:20. https://doi.org/10.1177/2397847317726352
81 Krebs KC, Lan Q (2003) Isolation and expression of a sterol carrier protein-2 gene from the yellow fever mosquito, *Aedesaegypti*. Insect Mol Biol. 12:51–60. https://doi.org/10.1046/j.1365-2583.2003.00386.x
82. Lan Q, Massey RJ (2004) Subcellular localization of mosquito sterol carrier protein-2 and sterol carrier protein-x. J Lipid Res 45:1468–1474. https://doi.org/10.1194/jlr.M400003-JLR200
83 Lan Q, Wessely V (2004) Expression of a sterol carrier protein-x gene in the yellow fever mosquito. Aedesaegypti. Insect. Mol Biol 13:519–529. https://doi.org/10.1111/j.0962-1075.2004.00510.x
84. Vyazunova I, Wessley V, Kim M, Lan Q (2007) Identification of two sterol carrier protein-2 like genes in the yellow fever mosquito, *Aedesaegypti*. Insect Mol Biol 16:305–314. https://doi.org/10.1111/j.1365-2583.2007.00729.x
85. Hariharan H, Al-Dhabi NA, Karuppiah P, Rajaram SK (2012) Microbial synthesis of selenium nanocomposite using *Saccharomyces cerevisiae* and its antimicrobial activity against pathogens causing nosocomial infection. Chalcogenide Lett 9:509–515
86. F.J. Ramos, S.C. Chen, M.G. Garelick, D.F. Dai, C.Y. Liao, K.H. Schreiber, V.L. MacKay, E.H. An, R. Strong, W.C. Ladiges, P.S. Rabinovitch, Rapamycin reverses elevated mTORC1 signaling in lamin A/C–deficient mice, rescues cardiac and skeletal muscle function, and extends survival. Sci Transl Med 4(2012)144ra103–144ra103. https://doi.org/10.1126/scitranslmed.3003802

87. Chudobova D, Simona C, Ruttkay B, Angel M, Katerina R, Kopel P, Jiri N, Sona G, Kynicky J, Vojtech K (2014) Comparison of the effects of silver phosphate and selenium nanoparticles on *Staphylococcus aureus* growth reveals potential for selenium particles to prevent infection. FEMS Microbiol Lett 35:195–201. https://doi.org/10.1111/1574-6968.12353
88. Nakayama S, Ojanguren AF, Fuiman LA (2011) Process-based approach reveals directional effects of environmental factors on movement between habitats. J Anim Ecol 80:1299–1304. https://doi.org/10.1111/j.1365-2656.2011.01859.x
89. Carson L, Bandara S, Joseph M, Green T, Grady T, Osuji G, Weerasooriya A, Ampim P, Woldesenbet S (2020) Green synthesis of silver nanoparticles with antimicrobial properties using *Phyladulcis* plant extract. Foodborne Pathog Dis 17:504–511. https://doi.org/10.1089/fpd.2019.2714
90. Khiralla GM, El-Deeb BA (2015) Antimicrobial and antibiofilm effects of selenium nanoparticles on some foodborne pathogens. LWT Food Sci Tech 63:1001–1007. https://doi.org/10.1016/j.lwt.2015.03.086
91. Karthik K, Dhanuskodi S, Gobinath C, Prabukumar S, Sivaramakrishnan S (2017) Photocatalytic and antibacterial activities of hydrothermally prepared CdO nanoparticles. J Mater Sci: Mater Electron 28:11420–11429. https://doi.org/10.1007/s10854-017-6937-z
92. Hosseinkhani PZ, Imani AM, Rezayi S, RezaeiZarchi MS (2011) Determining the antibacterial effect of ZnO nanoparticle against the pathogenic bacterium *higelladysenteriae*(type1). Int J Nano Dim 1:279–285. https://doi.org/10.7508/IJND.2010.04.00